

# Enantiomeric Polylactides at the Air–Water Interface: $\pi$ -A Isotherms and PM-IRRAS Studies of Enantiomers and Their Blend

Joy M. Klass, R. Bruce Lennox,\* and G. Ronald Brown†

Department of Chemistry, McGill University, 801 Sherbrooke St. West,  
Montréal, Québec H3A 2K6, Canada

Hélène Bourque and Michel Pézolet\*

Centre de recherche en sciences et ingénierie des macromolécules, Département de chimie,  
Université Laval, Cité Universitaire, Québec G1K 7P4, Canada

Received July 3, 2002. In Final Form: October 9, 2002

The surface pressure–area ( $\pi$ -A) isotherms of enantiomeric polylactides and their equimolar blend reveal differences in the appearance of features and compression rate effects. Surface potential data indicate that the poly(L-lactide) monolayer interacts differently than the 50:50 poly(L-lactide)/poly(D-lactide) blend film with the water subphase. In the case of the 50:50 blend at 25 °C, compression–expansion experiments confirm that the change in the monolayer is irreversible within the time frame of the experiment. In the poly(L-lactide) case, hysteresis is also observed, but the film readily reverts to its original state. Infrared spectra of the polymer monolayers at the air–water interface were obtained using the polarization–modulation infrared reflection–absorption spectroscopy (PM-IRRAS) technique. PM-IRRAS spectra of a compressed poly(L-lactide) monolayer are consistent with the polylactide helices lying in the plane of the air–water interface. No absorbances are observed in the PM-IRRAS spectra of poly(L-lactide) prior to the plateau in the  $\pi$ -A isotherms, suggesting that the helix formation is linked to the increase in surface density which accompanies film compression. The PM-IRRAS spectra establish that the conformation of the poly(L-lactide) helices with respect to the air–water interface is different than the conformation of the D/L blend helices.

## Introduction

Synthetic optically active polymers are divided into two classes: main-chain polymers in which the chiral centers are located along the polymer backbone and side-chain polymers in which the chiral centers are located in the pendent groups.<sup>1</sup> Polylactides belong to the former class and have been widely studied because of their biocompatibility.<sup>2,3</sup> Polylactides exist either as homopolymers (poly(L-lactide) or poly(D-lactide)), or as poly(D,L-lactide) copolymers in which L- and D- repeat units are present in the same chain.

It has been reported that poly(L-lactide) crystallizes as a 10<sub>3</sub> helix, the unit cell being pseudo-orthorhombic.<sup>4,5</sup> This is termed the  $\alpha$ -form. The  $\alpha$ -form was later reported to adopt a distorted 3<sub>1</sub> helix.<sup>6</sup> A 3<sub>1</sub> helix form has also been observed and is termed the  $\beta$ -form.<sup>7</sup>

A stereocomplex can result from the stereoselective association of optically active polyenantiomer chains during crystallization. Stereocomplexes have different physical properties (e.g., melting point, crystal structure, and morphology) than the constituent polyenantiomers. The term stereocomplex was first used by Liquori et al.<sup>8</sup>

to describe the association product between isotactic poly(methyl methacrylate) (*i*-PMMA) and syndiotactic PMMA (*s*-PMMA). *s*-PMMA and *i*-PMMA co-crystallize in a 2:1 stoichiometry yielding an X-ray diffraction pattern which is distinct from that of the isotactic material. The stability of this stereocomplex is attributed to the interlocking of syndiotactic molecules into channels formed by joining the helical grooves of neighboring isotactic helices. Other examples of polymers which undergo stereocomplexation in the bulk include poly(*tert*-butyl thiirane),<sup>9</sup> poly(benzyl glutamate),<sup>10</sup> poly( $\alpha$ -methyl  $\alpha$ -ethyl  $\beta$ -propiolactone) (PMEPL),<sup>11</sup> poly( $\beta$ -(dichloro-propyl)- $\beta$ -propiolactone) and poly( $\beta$ -(dichloroethyl)- $\beta$ -propiolactone).<sup>12</sup> It is important, however, to note that not all optically active polymers undergo stereocomplex formation. For example stereocomplexes in the bulk of poly(methylthiirane), poly(propylene oxide),<sup>13</sup> poly(isopropylethylene oxide),<sup>14</sup> poly( $\beta$ -hydroxybutyrate),<sup>15</sup> and poly( $\beta$ -ethyl- $\beta$ -propiolactone)<sup>16</sup> are not observed.

\* To whom correspondence should be addressed.

† Deceased June 19, 2001.

(1) Belfield, K. D.; Belfield, J. S. *Trends Polym. Sci.* **1995**, 3, 180.

(2) Anderson, J. M.; Shive, M. S. *Adv. Drug Delivery Rev.* **1997**, 28, 5.

(3) Maquet, V.; Jerome, R. *Mater. Sci. Forum* **1997**, 250, 15.

(4) De Santis, P.; Kovacs, A. J. *Biopolymers* **1968**, 6, 299.

(5) The present thought is that the 10<sub>3</sub> helix is unlikely. Lotz, B. Personal communication.

(6) Brizzolara, D.; Cantow, H.-J.; Diederichs, K.; Keller, E.; Domb, A. J. *Macromolecules* **1996**, 29, 191.

(7) Eling, B.; Gogolewski, S.; Pennings, A. J. *Polymer* **1982**, 23, 1587.

(8) Liquori, A. M.; Anzuino, G.; Coiro, V. M.; D'Alagni, M.; De Santis, P.; Savino, M. *Nature (London)* **1965**, 206, 358.

(9) Dumas, P.; Spassky, N.; Sigwalt, P. *Makromol. Chem.* **1972**, 156, 55.

(10) Fukuzawa, T.; Uematsu, I.; Uematsu, Y. *Polym. J. (Tokyo)* **1974**, 6, 537.

(11) Lavallée, C.; Prud'homme, R. E. *Macromolecules* **1989**, 22, 2438.

(12) Voyer, R.; Prud'homme, R. E. *Eur. Polym. J.* **1989**, 25, 365.

(13) Cesari, M.; Perego, G.; Marconi, W. *Makromol. Chem.* **1966**, 94, 194.

(14) Takahashi, Y.; Tadokoro, H.; Hirano, T.; Sato, A.; Tsuruta, T. *J. Polym. Sci., Polym. Phys. Ed.* **1975**, 13, 285.

(15) Yokouchi, M.; Chatani, Y.; Tadokoro, H.; Teranishi, K.; Tani, H. *Polymer* **1973**, 14, 267.

(16) Yokouchi, M.; Chatani, Y.; Tadokoro, H.; Tani, H. *Polym. J.* **1974**, 6, 248.

Stereocomplex formation initiated by mixing solutions of the enantiomeric polylactides was first reported by Ikada et al.<sup>17</sup> The resulting stereocomplex has a melting point 50 °C higher and a crystal structure distinct from that of the  $\alpha$ -form of poly(L-lactide). The stereocomplex exhibits a triclinic unit cell, the polyenantiomer chains being packed side-by-side in a parallel fashion, with poly(L-lactide) and poly(D-lactide) residues in a 1:1 ratio.<sup>18</sup> Ikada and co-workers have performed numerous studies on the formation, morphology, phase structure, crystalline structure, and degradability of this stereocomplex.<sup>19</sup> Differences in the solid state <sup>13</sup>C NMR spectra of poly(L-lactide) and the stereocomplex in the bulk have been attributed to the different helical arrangements of the polymers. Similarly, differences in the splitting of the Raman band due to the C=O stretching mode is attributed to differences in the conformation of the helical chains in the two materials.<sup>20</sup>

The properties of polymers in two dimensions (at an air–water interface) can be studied using the Langmuir film balance (LFB) technique. For example, a plateau observed in the  $\pi$ – $A$  isotherm of poly( $\beta$ -hydroxybutyrate) has been attributed to transformation from the amorphous state to a bilayer of helical molecules at the air–water interface.<sup>21</sup> PMMA monolayers have been studied in great detail using the LFB technique.<sup>22,23</sup> A plateau observed in the  $\pi$ – $A$  isotherm of  $i$ -PMMA has been attributed to a two-dimensional pseudocrystallization process resulting in the formation of a double helix.<sup>22</sup> This (inferred) structure is similar to that of  $i$ -PMMA crystallized in 3D. Infrared spectra of Langmuir–Blodgett (LB) multilayers of  $i$ -PMMA transferred at both pre- and post- plateau pressures of the isotherm are similar to the spectra of amorphous  $i$ -PMMA and bulk crystalline  $i$ -PMMA, respectively.<sup>24</sup> The compression-induced stereocomplexation of  $i$ -PMMA and  $s$ -PMMA at the air–water interface has also been reported.<sup>25</sup> In this case a transition in the  $\pi$ – $A$  isotherm of mixed monolayers of  $i$ -PMMA and  $s$ -PMMA corresponds to the stereocomplexation process.

A number of studies involving monolayers at the air–water interface of poly(D,L-lactic acid),<sup>26</sup> copolymers with glycolide,<sup>27–29</sup> and mixed monolayers with poly(vinyl alcohol),<sup>30,31</sup> bovine serum albumin,<sup>32</sup> calcitonin,<sup>33</sup> and

cyclosporin<sup>34</sup> have been reported. To investigate the suitability of these materials as stabilizers in emulsion polymerization, mixed monolayers of poly(vinyl alcohol) and poly(D,L-lactic acid) were studied at the air–water and dichloromethane–water interfaces.<sup>30,31</sup> Mixed monolayers of poly(D,L-lactide) and either cyclosporin or calcitonin were studied to investigate the feasibility of using cyclosporin and calcitonin-loaded polymer spheres for drug delivery.<sup>33,34</sup> The kinetics of acidic, basic,<sup>35</sup> and enzymatic hydrolyses<sup>36</sup> of monolayers of poly(D,L-lactide) at the air–water interface have also been reported. The hydrolysis kinetics of poly(L-lactide) have also been studied.<sup>37</sup> However the monolayer structure of the enantiomeric polylactides has not been studied in detail.

Given this background, we have undertaken a study of the comparative behavior of the homopolylactides and mixed polyenantiomers at the air–water interface. Polarization-modulation infrared reflection–absorption spectroscopy (PM-IRRAS) has also been used to study the structure of the poly(L-lactide) monolayers in situ at the air–water interface as a function of surface pressure. The correlation between the isotherm features and PM-IRRAS spectra allow one to describe relationships between the 2D and 3D states of these materials.

IRRAS was originally employed to study lipid monolayers at the air–water interface by Dluhy and co-workers.<sup>38,39</sup> However, the application of IRRAS to the in situ investigation of monolayers at the air–water interface has been severely limited by the weakness of the infrared bands, the poor reflectivity of water and, most significantly, by the strong spectral interference of water vapor absorptions in the 1400–1800 cm<sup>−1</sup> region.<sup>40</sup> Unfortunately, conformation-sensitive bands due to the amide I, amide II, and carbonyl vibration of polyamides and polyesters arise in this spectral window. This latter problem has been partially overcome by using either D<sub>2</sub>O<sup>40,41</sup> as a subphase or the polarization-modulation<sup>42–50</sup> technique. Polarization-modulation IRRAS (PM-IRRAS) is especially powerful because the detected signal is differential in nature. Spectra are almost unaffected by the isotropic absorptions of the sample environment and the sign of a band is directly related to the orientation of the transition moments with respect to the plane of the water surface.

(17) Ikada, Y.; Jamshidi, K.; Tsuji, H.; Hyon, S.-H. *Macromolecules* **1987**, *20*, 904.

(18) Okihara, T.; Tsuji, M.; Kawaguchi, A.; Katayama, K.-I.; Tsuji, H.; Hyon, S.-H.; Ikada, Y. *J. Macromol. Sci., Phys.* **1991**, *B30*, 119.

(19) Tsuji, H.; Ikada, Y. *Polymer* **1999**, *40*, 6699 and previous papers in the series.

(20) Kister, G.; Cassanas, G.; Vert, M. *Polymer* **1998**, *39*, 267.

(21) Lambeck, G.; Vorenkamp, E. J.; Schouten, A. J. *Macromolecules* **1995**, *28*, 2023.

(22) Brinkhuis, R. H. G.; Schouten, A. J. *Macromolecules* **1991**, *24*, 1487.

(23) Brinkhuis, R. H. G.; Schouten, A. J. *Macromolecules* **1992**, *25*, 5692.

(24) Brinkhuis, R. H. G.; Schouten, A. J. *Macromolecules* **1991**, *24*, 1496.

(25) Brinkhuis, R. H. G.; Schouten, A. J. *Macromolecules* **1992**, *25*, 2725.

(26) Boury, F.; Gulik, A.; Dedieu, J. C.; Proust, J. E. *Langmuir* **1994**, *10*, 1654.

(27) Miñones, J.; Iribarnegaray, E.; Varela, C.; Vila, N.; Conde, O.; Cid, L.; Casas, M. *Langmuir* **1992**, *8*, 2781.

(28) Boury, F.; Olivier, E.; Proust, J. E.; Benoit, J. P. *J. Colloid Interface Sci.* **1993**, *160*, 1.

(29) Vila Romeu, N.; Miñones, J.; Iribarnegaray, E.; Conde, O.; Casas, M. *Colloid Polym. Sci.* **1997**, *275*, 580.

(30) Boury, F.; Olivier, E.; Proust, J. E.; Benoit, J. P. *J. Colloid Interface Sci.* **1994**, *163*, 37.

(31) Boury, F.; Ivanova, T.; Panaiotov, I.; Proust, J. E.; Bois, A.; Richou, J. *J. Colloid Interface Sci.* **1995**, *169*, 380.

(32) Boury, F.; Ivanova, T.; Panaiotov, I.; Proust, J. E. *Langmuir* **1995**, *11*, 599.

(33) Vila Romeu, N.; Miñones Trillo, J.; Conde, O.; Casas, M.; Iribarnegaray, E. *Langmuir* **1997**, *13*, 76.

(34) Vila Romeu, N.; Miñones, J.; Conde, O.; Iribarnegaray, E.; Casas, M. *J. Colloid Interface Sci.* **1997**, *185*, 77.

(35) Ivanova, T.; Panaiotov, I.; Boury, F.; Proust, J. E.; Benoit, J. P.; Verger, R. *Colloids Surf. B: Biointerfaces* **1997**, *8*, 217.

(36) Ivanova, T.; Panaiotov, I.; Boury, F.; Proust, J. E.; Verger, R. *Colloid Polym. Sci.* **1997**, *275*, 449.

(37) Lee, W.-K.; Gardella, J. A. *Langmuir* **2000**, *16*, 3401.

(38) Dluhy, R. A.; Cornell, D. G. *J. Phys. Chem.* **1985**, *89*, 3195.

(39) Hunt, R. D.; Mitchell, M. L.; Dluhy, R. A. *J. Mol. Struct.* **1989**, *214*, 93.

(40) Mendelsohn, R.; Brauner, J. W.; Gericke, A. *Annu. Rev. Phys. Chem.* **1995**, *46*, 305.

(41) Flach, C. R.; Gericke, A.; Mendelsohn, R. *J. Phys. Chem. B* **1997**, *101*, 58.

(42) Blaudez, D.; Buffeteau, T.; Cornut, J. C.; Desbat, B.; Escafre, N.; Pézolet, M.; Turlet, J. M. *Appl. Spectrosc.* **1993**, *47*, 869.

(43) Blaudez, D.; Buffeteau, T.; Cornut, J. C.; Desbat, B.; Escafre, N.; Pézolet, M.; Turlet, J. M. *Thin Solid Films* **1994**, *242*, 146.

(44) Blaudez, D.; Turlet, J.-M.; Dufourcq, J.; Bard, D.; Buffeteau, T.; Desbat, B. *J. Chem. Soc., Faraday Trans.* **1996**, *92*, 525.

(45) Cornut, I.; Desbat, B.; Turlet, J.-M.; Dufourcq, J. *Biophys. J.* **1996**, *70*, 305.

(46) Mao, L.; Ritcey, A.; Desbat, B. *Langmuir* **1996**, *12*, 4754.

(47) Payan, S.; Desbat, B.; Destrade, C.; Nguyen, H. T. *Langmuir* **1996**, *12*, 6627.

(48) Castano, S.; Desbat, B.; Cornut, I.; Méléard, P.; Dufourcq, J. *Lett. Peptide Sci.* **1997**, *4*, 195.

(49) Xiao, Y.; Bourque, H.; Pézolet, M.; Ritcey, A. M. *Thin Solid Films* **1998**, *327–329*, 299.

(50) Dicko, A.; Bourque, H.; Pézolet, M. *Chem. Phys. Lipids* **1998**, *96*, 125.

We have recently reported the use of the PM-IRRAS technique to investigate the structure of monolayers of the poly(L-lactide)/poly(D-lactide) stereocomplex at the air–water interface.<sup>51</sup> In contrast to PM-IRRAS, several other frequently used in situ techniques (e.g., X-ray reflectivity, neutron reflectivity, ellipsometry, Brewster angle microscopy, fluorescence microscopy) do not directly provide molecular details. FT-IR on the other hand offers molecular details about hydrogen bonding, bond angles, and is amenable to in situ observation when used in the PM mode. In our previous study, the PM-IRRAS methodology was discussed and the relevant spectral assignments made.<sup>51</sup> The molecular details made evident from this PM-IRRAS study are otherwise unobtainable.

### Experimental Section

**Materials.** Poly(L-lactide) was prepared by the ring-opening polymerization of L-(–)-lactide (Purac Biochem BV, Gorinchem, The Netherlands) with stannous octoate (Sigma Chemical Co., St. Louis, MO) as the catalyst and lauryl alcohol as the initiator. The reaction was performed under vacuum at 140 °C for 6 h according to the method of Kleine and Kleine.<sup>52</sup> Poly(D-lactide) was prepared from D-(+)-lactide (Purac Biochem BV, Gorinchem, The Netherlands) by the same method. The polymers were purified by reprecipitation, using methylene chloride as the solvent and methanol as the precipitant.

The weight-average molecular weights of the polymers in dioxane were determined by gel permeation chromatography at 308 K, using a series of Waters Styragel HR columns (Waters Corp., Milford, MA). Values of  $1.0 \times 10^5$  for the poly(L-lactide) and  $1.2 \times 10^5$  for the poly(D-lactide) were obtained using polystyrene standards. The molecular weight distributions (polydispersities ( $M_w/M_n$ )) were 1.8 and 2.9 respectively.

**Langmuir Film Balance Measurements.** Surface pressure–area isotherms were obtained using either a KSV 3000 film balance ( $15 \times 58$  cm) (KSV Instruments Ltd., Helsinki, Finland) equipped with dual barriers and a Wilhelmy plate sensing device, or a Lauda model FW-2 film balance (Lauda, Germany), equipped with one moving barrier and a lateral pressure sensing device. The subphase temperatures were maintained using a Haake D circulation temperature controller (Haake, Germany). Subphase water (18 M $\Omega$ /cm) was prepared by passing house distilled water through a Milli-Q system (Millipore, Bedford, MA) equipped with an organic residue cartridge.

Polymer stock solutions were prepared using chloroform (HPLC grade) to give final concentrations of 0.4–0.5 mg/mL. In a typical experiment, polymer films were formed by spreading 40–50  $\mu$ L of the stock solution dropwise over the surface. Compression was initiated after a delay of 15 min to allow evaporation of the spreading solvent. Experiments were performed using solutions of poly(L-lactide), poly(D-lactide) and the D/L blend. Isotherms were obtained at temperatures ranging from 5 to 35 °C. The compression time was typically 30 min.

Hysteresis experiments involved a pause time of 1 min at the target (compression) surface pressure and a 1 h pause at the expansion surface pressure before recompression commenced, unless otherwise specified. The compression and expansion rates for a given hysteresis experiment were constant.

The surface potential was recorded at the same time as the surface pressure measurements. Surface potential was recorded using a KSV 5000SP vibrating plate capacitor surface potential meter (KSV Instruments Ltd., Helsinki, Finland). The upper electrode vibrates with a frequency of about 80–120 Hz. The lower platinum electrode was placed under the surface of the water subphase. The measuring range of the meter is  $\pm 10$  V and the manufacturer's stated accuracy is  $\pm 5$  mV.

**PM-IRRAS Measurements.** PM-IRRAS experiments were performed using a home-built Langmuir trough ( $36.1$  cm  $\times$   $5$  cm) equipped with a filter paper Wilhelmy plate sensor and coupled

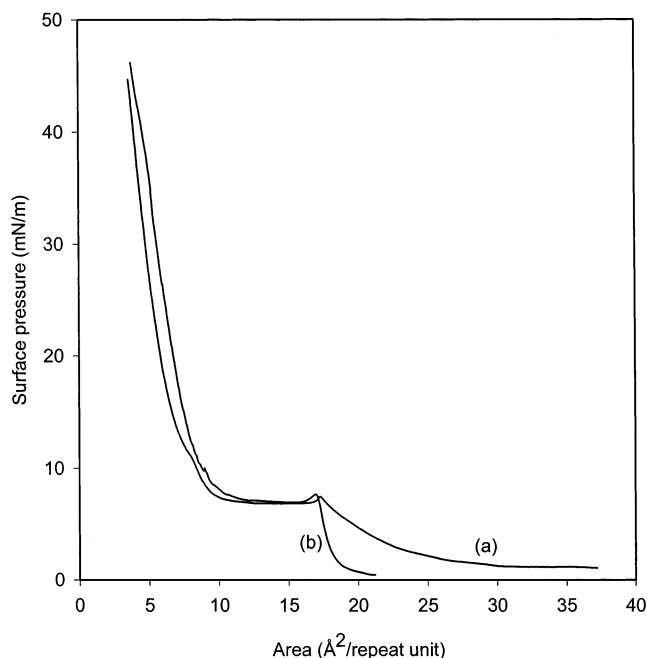


**Figure 1.** Surface pressure–area isotherms of spread monolayers of (a) poly(L-lactide) and (b) the 50:50 blend of poly(L-lactide) and poly(D-lactide) recorded at 35 °C.

to a Nicolet 850 FTIR spectrometer. The PM-IRRAS setup has been described in detail elsewhere.<sup>51</sup> Monolayers were spread from chloroform (HPLC grade). Solutions were prepared by dissolving the polymer directly in the solvent at about 0.2 mg/mL. Spectra of the covered  $S(d)$  and uncovered  $S(o)$  water surface were acquired at an angle of incidence of 76° and at a resolution of 4  $\text{cm}^{-1}$  and by co-adding 400 scans unless otherwise stated.

All spectra are reported as normalized difference PM-IRRAS spectra,  $\Delta S/S = (S(d) - S(o))/S(o)$  with baseline correction. SpectraCalc software (Galactic Industries Corp.) was used to analyze spectra.

**Conventional IR Spectra.** IR spectra were recorded on a Bruker IFS48 spectrometer. The samples were incorporated into KBr pellets.

### Results and Discussion

**Surface Pressure–Area Isotherms.** Since the  $\pi$ – $A$  behavior of poly(L-lactide) is identical to that of poly(D-lactide), the discussion will focus on the comparison of one polyenantiomer (poly(L-lactide)) with the D/L blend. The surface pressure–area isotherms of poly(L-lactide) and a D/L blend at 35 °C are rich in detail and differ from one another in interesting ways (Figure 1). The poly(L-lactide) isotherm exhibits a high compressibility region, a pre-plateau feature, a sharp knee (a term generally used to describe the onset of a plateau) followed by a relatively horizontal plateau. The sharp knee is often seen in the isotherms of polymer monolayers. A post-plateau inflection point and a low compressibility region follow on from these features as the compression proceeds. The isotherm of the D/L blend displays similar features to that of poly(L-lactide) except that the rise in  $\pi$ , from onset to the knee, is significantly steeper in the D/L blend than for the poly(L-lactide). Moreover, the knee is also less pronounced in the case of the D/L blend than in poly(L-lactide).

The isotherm features suggest several possibilities. Since the polylactides are known to exist in a helical conformation in the crystalline state, a random 2D chain-to-helix transition may be associated with the plateau. Helices may also be present at large surface areas (before

(51) Bourque, H.; Laurin, I.; Pézolet, M.; Klass, J. M.; Lennox, R. B.; Brown, G. R. *Langmuir* **2001**, *17*, 5842.

(52) Kleine, J.; Kleine, H.-H. *Makromol. Chem.* **1959**, *30*, 23.



the plateau occurs) as in the case of polypeptide films.<sup>53–57</sup> If helices are indeed present prior to the plateau, the plateau may arise from bilayer formation, as reported for monolayers of  $\alpha$ -helical polypeptides.<sup>53–56</sup> The isotherm features of the D/L blend may arise from either the mixing that takes place in the solution prior to spreading at the air–water interface or to the compression process itself. Finally, the differences between the polyenantomer and D/L blend isotherms may reflect known differences observed in the bulk materials. As in the vast majority of monolayer studies,  $\pi$ – $A$  curves provide tantalizing suggestions of surface pressure-related phenomena with, however, little more than projected areas on which to base assignments. Given the distinctions obvious in the  $\pi$ – $A$  isotherms, we turned to a variety of experiments (e.g., surface potential, compression–expansion cycles and the in situ PM-IRRAS technique) in order to differentiate between the monolayers of the polyenantomer and D/L blend in molecular terms.

In the case of the poly(L-lactide) isotherm, the gradual surface pressure increase in the pre-plateau region is suggestive of a compressible, fluid-like film in this region. In the 50:50 D/L blend case, the rapid rise in  $\pi$  (indicative of low compressibility) in the preplateau region of the isotherm suggests that the film is considerably stiffer than in the case of the poly(L-lactide).

To see what form the  $\pi$ – $A$  isotherm adopts from the separate (rather than pre-mixed) addition of the two polyenantomers, poly(D-lactide) and poly(L-lactide) were applied at opposite ends of the water surface. The resulting isotherms (30 and 360 min compression times) are similar to those of the individual homopolymers. Evidently, mixing of the two components on the surface does not occur when the two materials are individually applied. In a second “mixing” configuration, a Teflon divider with a small channel in the middle was used to divide the water surface into two equal sections. A glass coverslip was used to block the channel so as to keep the two surfaces separate. A poly(L-lactide) solution was spread on one side of the divide and a poly(D-lactide) solution was spread on the other side. After the solvent was allowed to evaporate, the glass coverslip was removed and compression (using two moving barriers) of both films was initiated. Again the resulting isotherm was similar to those of the homopolymers, showing that mixing using this method does not occur. In the case of the D/L blend, interactions which occur prior to spreading on the water surface, clearly determine the resulting film structure.

**Surface Potential Measurements.** The surface potential  $\Delta V$ – $A$  curves of both poly(L-lactide) and the D/L blend (Figure 2) exhibit increases in  $\Delta V$ . Upon compression, a change in the slope of the  $\Delta V$ – $A$  plots occurs at the areas corresponding to the beginning of the plateau in the  $\pi$ – $A$  isotherms. Additional information is obtained if the perpendicular dipole moment ( $\mu_{\perp}$ ) per residue is plotted as a function of the residual area, where

$$\mu_{\perp} = \frac{\Delta V A}{12\pi} \quad (1)$$

$A$  is the area per residue (in  $\text{\AA}^2/\text{residue}$ ),  $\Delta V$  is the surface potential in mV, and  $\mu_{\perp}$  is expressed in mD. The  $12\pi$  factor is a conversion factor between cgs and mks units.

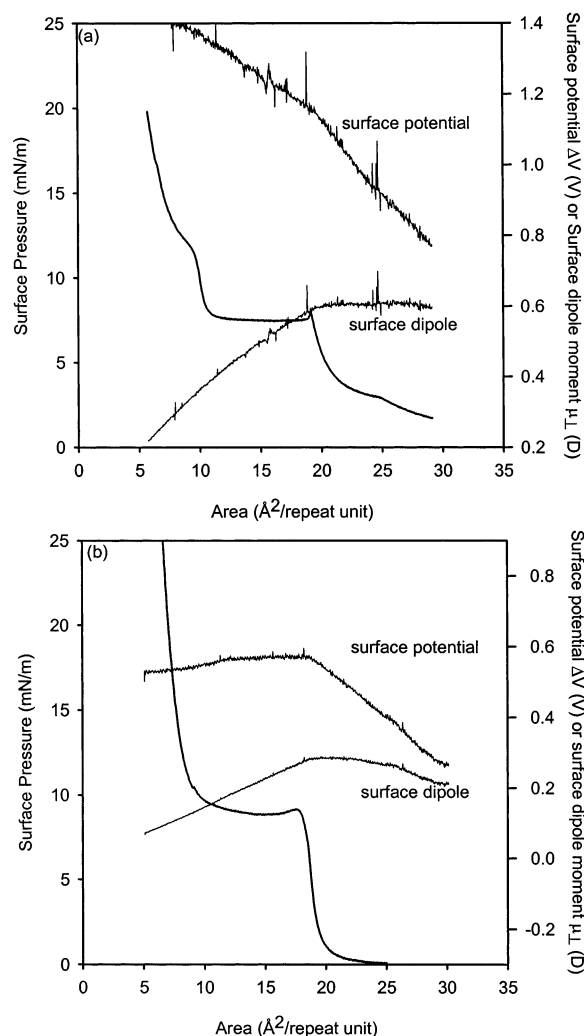


**Figure 2.** Surface potential of (a) poly(L-lactide) and the (b) D/L blend at 25 °C.

Differences between the orientation of the ester groups in the polymers' backbone and the differences in orientation of the hydrophobic  $\text{CH}_3$  groups in a  $3_1$  helix and a  $10_3$  helix (or a distorted  $3_1$  helix) would affect how the films interact with the dipoles of the underlying water subphase. This would result in differences in the  $\mu_{\perp}$  of the poly(L-lactide) and the D/L blend. Interestingly, the  $\pi$ – $A$  isotherm features at areas of 25 and  $9 \text{ \AA}^2/\text{residue}$  for the poly(L-lactide) are not apparent in the surface potential data. It is therefore unlikely that the  $\pi$ – $A$  features at these areas are due to a reorientation of molecules at the air–water interface.

Given that a helical molecule can have a substantial dipole along its axis,  $\mu_{\perp}$  differences may also arise from differences in orientation of helices with respect to the air–water interface. If an array of helices is oriented in the plane of the surface there will be no  $\mu_{\perp}$  component associated with the helices themselves. A change in the surface dipole linked to such a parallel orientation is thus most likely due to the reorientation of water molecules at the water–polymer interface. Such is the case for poly-alanine helices, where the reorientation of water molecules caused by their interaction with other polypeptide helices has been reported.<sup>57</sup> Such an assignment assumes that no contribution from distortion of the  $\alpha$ -helix (or its side chains) occurs under compression. It is not however possible at this stage to distinguish the relative contribu-

(53) Malcolm, B. R. *Polymer* **1966**, 7, 595.

(54) Malcolm, B. R. *Proc. R. Soc. A* **1968**, 305, 363.

(55) Malcolm, B. R. *J. Polym. Sci., Part C* **1971**, 34, 87.

(56) Malcolm, B. R. *Prog. Surf. Membr. Sci.* **1973**, 7, 183.

(57) Lavigne, P.; Tancrede, P.; Lamarche, F.; Max, J.-J. *Langmuir* **1992**, 8, 1988.

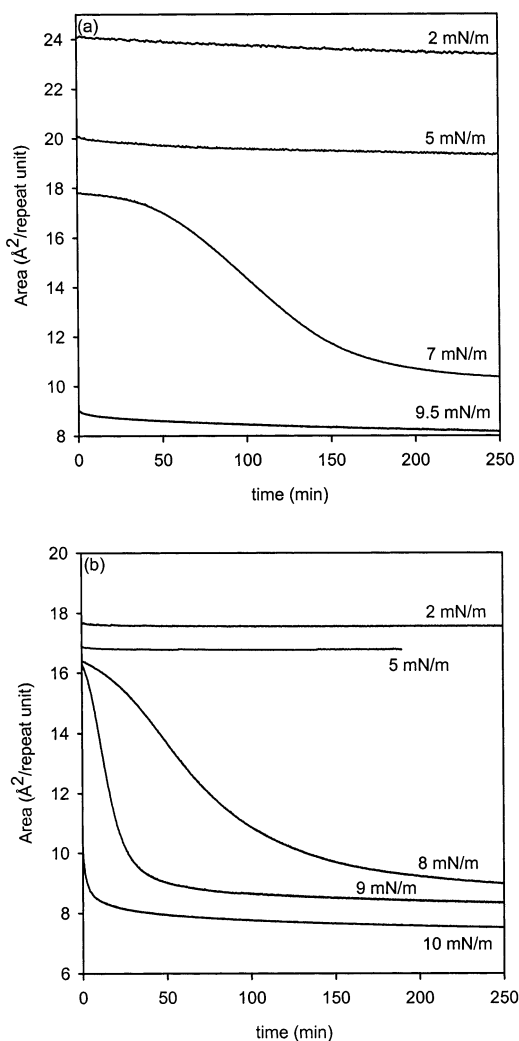


**Figure 3.** Isobars of (a) poly(L-lactide) and (b) the D/L blend at 25 °C.

tions of these two situations. The PM-IRRAS experiment (vide infra) does however help to clarify the details of the monolayer structure.

**Isobars.** To complement the information described above, isobaric stabilization experiments were performed. In these experiments, the surface pressure is maintained at a constant value and one monitors the area changes arising from changes in the film. Figure 3 shows the isobars obtained at several surface pressure values. At surface pressure values prior to the knee and after the plateau, the area per repeat unit values at which the monolayer stabilizes correspond to the area values of the target surface pressure on  $\pi$ - $A$  isotherms. At surface pressure values close to those of the knee region of the isotherms, "S-shaped" isobars are observed. The final areas of isobars thus obtained do not correspond to those obtained with the  $\pi$ - $A$  isotherms. Instead, the area (per repeat unit) values correspond to the end of the isotherm plateau (ca. 8 Å²/repeat unit). This difference between isobars most probably arises from differences in the kinetics of association processes in the films. Indeed, the occurrence of S-shaped curves supports a model involving an autoacceleration of the film transition process.

Attempts to differentiate the processes which may occur in Langmuir films have been previously assessed using the Avrami crystallization formalism.<sup>22,58–60</sup> Gabrielli and

Guarini<sup>58</sup> also tested relationships previously used in studies of solid decomposition.<sup>61,62</sup> According to these reports none of these relationships yield a good fit over the entire range of experimental data. Avrami plots of the data obtained here yield complex curves consisting of several regions. These fits are inconclusive as the Avrami exponents are non-integral for the initial regions and are fractional for subsequent regions.

**Hysteresis.** The isobar experiments revealed that differences in the response kinetics of the poly(L-lactide) and the D/L blend may be important. The effect of repetitive compression–expansion cycles directly assesses the relationships between film structure and kinetics effects.

Figure 4 shows the compression–expansion curves for poly(L-lactide) and the D/L blend at 25 °C. At area values well below the knee, the isotherms of both poly(L-lactide) and the D/L blend are reversible. At these areas, each film expands as fast as the barrier expands (approximately 1 (Å²/residue)/min).

On compression to areas close to the knee, the expansion of the poly(L-lactide) monolayer is not reversible (with respect to the experimental rate of expansion of the barrier). However, a recompression of the poly(L-lactide) (after a pause of 60 min) yields an isotherm which is superimposable upon the initial compression isotherm (Figure 4a). The D/L blend film also expands more slowly than the rate of expansion of the barrier (approximately 1 (Å²/residue)/min), but a subsequent compression isotherm (after a pause of 60 min) is not superimposable upon the first compression isotherm (Figure 4b).

At areas beyond the plateau, the compression of the poly(L-lactide) monolayer is not instantaneously reversible, but after expansion and a pause time of 60 min, the second compression isotherm of poly(L-lactide) coincides with the first compression isotherm (Figure 4c). In the case of the D/L blend, the film expands more slowly than the rate of barrier expansion and the recompression isotherm (after a pause of 60 min) is markedly different from that of the original compression isotherm (Figure 4d). This marked difference in hysteresis demonstrates that the monolayers of poly(L-lactide) and the D/L blend differ in terms of their intermolecular interactions.

This compression–expansion behavior of poly(L-lactide) is similar to that observed in the monolayer crystallization of *i*-PMMA,<sup>22</sup> while the hysteresis of the D/L blend is similar to that observed in the monolayer stereocomplex formed from *i*- and *s*-PMMA.<sup>63</sup>

**Compression Rate Dependence.** Both the isobar experiments and the compression–expansion experiments suggest that kinetics effects are important in these materials. The effect of compression rate on the shape of the isotherms and position of the plateau gives further insight into the nature of the process occurring during compression. The D/L blend isotherm exhibits decreasing surface pressure with decreasing compression rate, suggesting that the plateau is associated with a slow process (results not shown). The overshoot at the knee becomes more pronounced at low compression rates.

(58) Gabrielli, G.; Guarini, G. G. T. *J. Colloid Interface Sci.* **1978**, *64*, 185.

(59) Wang, L. F.; Kuo, J. F.; Chen, C. Y. *Mater. Chem. Phys.* **1995**, *40*, 197.

(60) Arslanov, V. V.; Sheinina, L. S.; Bulgakova, R. A.; Belomestnykh, A. V. *Langmuir* **1995**, *11*, 3953.

(61) Garner, W. E. *Chemistry of the Solid State*; Butterworths: London, 1955.

(62) Young, D. A. *Decomposition of Solids*; Pergamon: Oxford, England, 1966.

(63) Brinkhuis, R. H. G.; Schouten, A. J. *Macromolecules* **1992**, *25*, 2732.

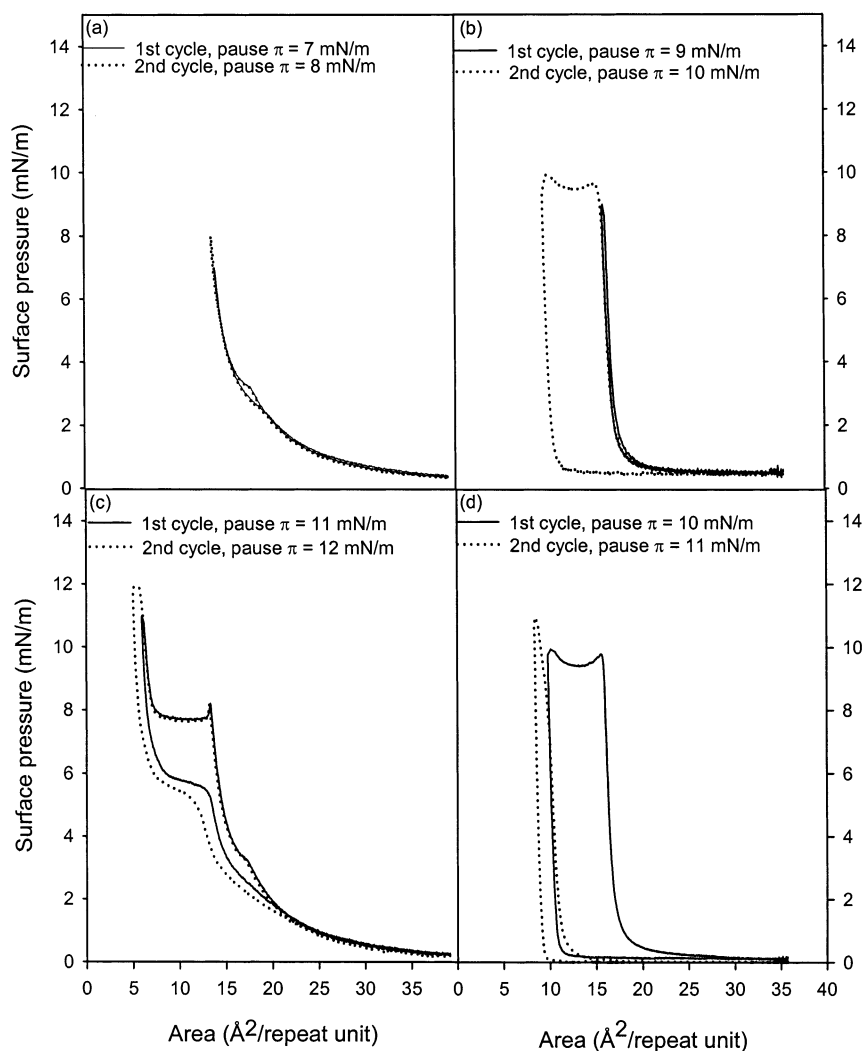


**Figure 4.** Compression-expansion curves at 25 °C of (a) poly(L-lactide) (first cycle, pause  $\pi = 7$  mN/m; second cycle, pause  $\pi = 8$  mN/m), (b) the D/L blend (first cycle, pause  $\pi = 9$  mN/m; second cycle, pause  $\pi = 10$  mN/m), (c) poly(L-lactide) (first cycle, pause  $\pi = 11$  mN/m, second cycle, pause  $\pi = 12$  mN/m), and (d) the D/L blend (first cycle, pause  $\pi = 10$  mN/m; second cycle, pause  $\pi = 11$  mN/m).

**PM-IRRAS Spectra.** The PM-IRRAS technique is used to determine the molecular origins of the differences between the monolayers of the polylactide polyenantiomers and D/L blend described above. Comparison of the spectra of the bulk poly(L-lactide) and the bulk spectrum of the D/L blend (peak assignments based on the data of Kister et al.<sup>20,64</sup>) reveals small differences between the two. For example, the homopolymer carbonyl stretch is at 1759  $\text{cm}^{-1}$  and the stereocomplex carbonyl stretch is at 1757  $\text{cm}^{-1}$ .

The PM-IRRAS spectrum of a poly(L-lactide) monolayer at the air–water interface at 35 °C ( $\pi = 20$  mN/m) and the FT-IR spectrum of the bulk material offer an interesting comparison (Figure 5). The bands due to the  $\delta_{\text{as}}(\text{CH}_3)$  and  $\delta_{\text{s}}(\text{CH}_3)$  that are present in the spectrum of the bulk sample at 1456 and 1384  $\text{cm}^{-1}$ , respectively, are very weak in the PM-IRRAS spectrum. Similarly, the bands due to the  $\nu_{\text{as}}(\text{CH}_3)$ ,  $\nu_{\text{s}}(\text{CH}_3)$ , and  $\nu(\text{CH})$  vibrations, (which appear at 2997, 2942, and 2882  $\text{cm}^{-1}$  respectively) are not apparent in the PM-IRRAS spectrum, even at a modulator setting of 3000  $\text{cm}^{-1}$  (results not shown). This is probably because the transition moments associated with these bands are isotropically oriented with respect to the surface normal. On the other hand, the bands due to the  $\nu_{\text{as}}(\text{COC})$ ,  $\nu_{\text{s}}(\text{COC})$  and  $\nu(\text{CH}_3)$  modes appear as strong positive bands in the PM-IRRAS spectrum indicating that their transition

moments are preferentially oriented parallel to the air–water interface.

Whereas the band due to the carbonyl stretching mode is observed as a strong peak at 1759  $\text{cm}^{-1}$  for the bulk poly(L-lactide), it is split into two bands in the PM-IRRAS spectrum as in the case of the PM-IRRAS spectrum of the stereocomplex.<sup>51</sup> By comparison with the Raman spectrum of semicrystalline poly(L-lactide), the positive  $\nu(\text{C=O})$  peak (1755  $\text{cm}^{-1}$ ) is assigned to the A mode (transition moment along the helix axis) and the negative  $\nu(\text{C=O})$  peak (1765  $\text{cm}^{-1}$ ) is assigned to the E mode (transition moment perpendicular to the helix axis). The fact that the transition moment associated with the E mode is perpendicular to the plane of the film has been associated with the intermolecular coupling between the polylactide helices in the plane of the film at the air–water interface. The selective attenuation of the in-plane component of the E mode leaves the out-of-plane component unaffected.<sup>20,51</sup> Although the two components of the  $\nu(\text{C=O})$  vibration cannot be resolved in the infrared spectrum of the bulk sample, the orientation selection rule of the PM-IRRAS technique<sup>43</sup> leads to absorbances of the opposite sign for the A and E modes of the carbonyl stretch of the helix.

(64) Kister, G.; Cassanas, G.; Vert, M.; Pauvert, B.; Térol, A. *J. Raman Spectrosc.* **1995**, *26*, 307.

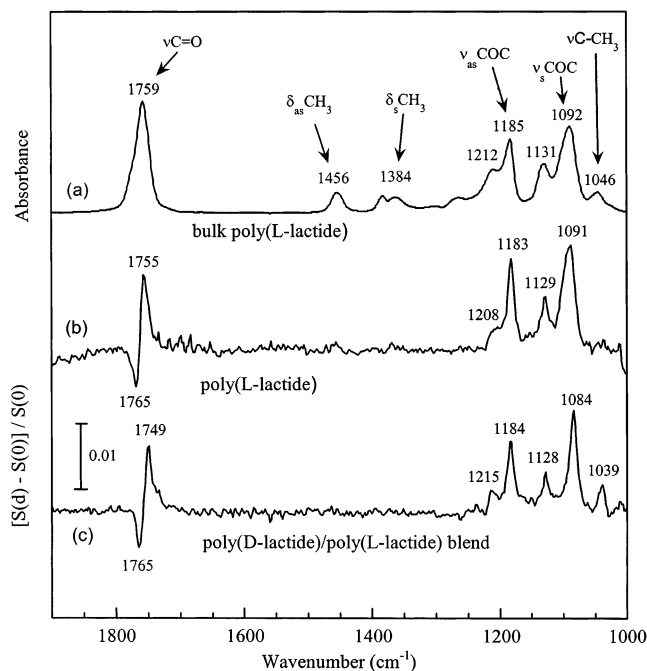


**Figure 5.** Comparison of the (a) FT-IR spectrum of bulk poly(L-lactide), (b) PM-IRRAS spectrum of poly(L-lactide) at high surface pressure, and (c) PM-IRRAS spectrum of the D/L blend at high surface pressure.

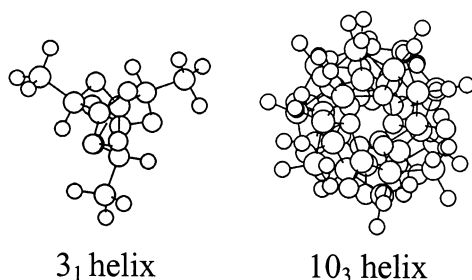


**Figure 6.** Difference between the arrangement of the methyl groups for the 10<sub>3</sub> and 3<sub>1</sub> helices according to Okihara et al.<sup>18</sup>

The PM-IRRAS spectrum of poly(L-lactide) thus indicates clearly that the helical poly(L-lactide) molecules exist in the post-plateau region of the isotherm with their axes parallel to the interface.

It is interesting to compare the PM-IRRAS spectra of the poly(L-lactide) and the D/L blend. Figure 5 reveals that the wavenumber difference between the A and E modes is much more pronounced for the blend (16 cm<sup>-1</sup>) than for the poly(L-lactide) (10 cm<sup>-1</sup>). In addition, the C-CH<sub>3</sub> stretch at 1046 cm<sup>-1</sup>, clearly observed in the spectrum of bulk poly(L-lactide) and in the PM-IRRAS spectrum of the D/L blend, is not observed in the PM-IRRAS spectrum of poly(L-lactide). According to the models of Okihara et al.<sup>18</sup> (Figure 6), the 1046 cm<sup>-1</sup> due to the C-CH<sub>3</sub> stretching mode should be quite weak in the PM-IRRAS spectrum of a 10<sub>3</sub> helix lying flat on the water surface. This is because the CH<sub>3</sub> groups are symmetrically arranged when viewed from a perspective looking down the helix axis. The absence of the C-CH<sub>3</sub> stretch thus supports the assignment of a 10<sub>3</sub> poly(L-lactide) helix at the air-water interface. On the other hand, the C-CH<sub>3</sub> stretch is observed in the PM-IRRAS spectra of the D/L blend<sup>51</sup> at 1039 cm<sup>-1</sup> (Figure 5), consistent with the existence of the 3<sub>1</sub> helix according to the models of Okihara et al.<sup>18</sup> (Figure 6).

The carbonyl stretch (1755, 1765 cm<sup>-1</sup>), COC stretch (1183, 1206 cm<sup>-1</sup>), and CH<sub>3</sub> rocking bands (1129 cm<sup>-1</sup>) in

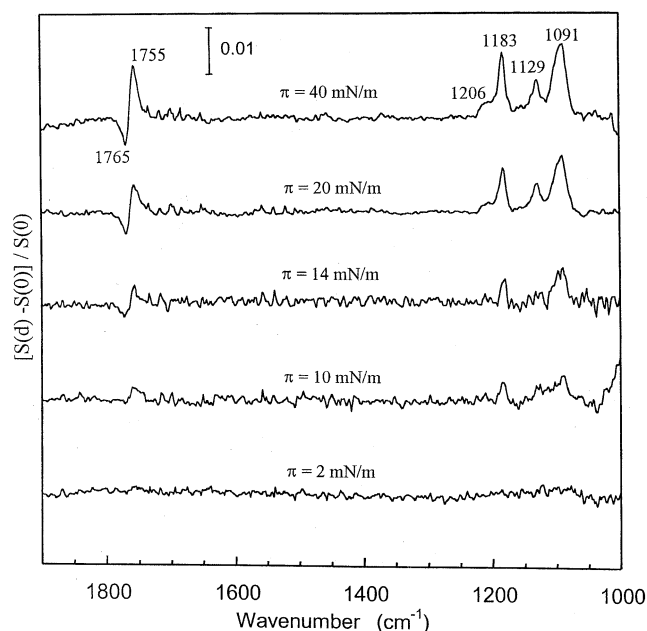


**Figure 7.** Normalized PM-IRRAS spectra of poly(L-lactide) spread as a monolayer at the air-water interface at 35 °C as a function of monolayer compression. Spectral intensity increases with decreasing molecular area.

the PM-IRRAS spectra of the poly(L-lactide) monolayer exhibit increased intensity with increasing surface density of lactide residues (Figure 7). No spectral absorbances are observed at surface areas greater than that of the knee, whereas at surface areas less than that of the knee, bands are observed. Furthermore, the spectral signature of a helix is evident in spectra obtained beyond the knee.

In the case of poly(L-lactide), the onset of the absorbance bands in the PM-IRRAS spectra beyond the knee suggest that there is an *induced* ordering of the molecules with increased surface density. The appearance of the helix spectral signature at the plateau suggests the existence of compression-induced helices at the air-water interface. This is similar to a report of compression-induced helices (in the case of *i*-PMMA<sup>22</sup>) using IR spectra of the associated LB films.<sup>24</sup> In comparison, absorbance bands are evident even at low surface pressures in the PM-IRRAS spectra of the D/L blend.<sup>51</sup> Preliminary Brewster angle microscopy measurements performed simultaneously with compression-expansion experiments of the D/L blend in fact suggest the formation of rigid, incompressible structures at high surface pressures. Further experiments will be performed to compare the homopolymer with the blend.

## Conclusions

Poly(L-lactide) and poly(D-lactide) produce identical  $\pi$ - $A$  isotherms at the air-water interface. Their behavior at the air-water interface differs however from that of the D/L blend. The rise in  $\pi$  from the onset to the knee of the polyenantiomer isotherms suggest the existence of fluid-like films, while the isotherm of the D/L blend suggests a stiffer film. The presence of the overshoot feature suggests that there is a nucleation process occurring at a well-defined area. "S-shaped" isobars support a model involving autoacceleration of a surface association process. Differences in surface potentials (and surface dipoles) of poly(L-lactide) and the D/L blend suggest that the molecules are oriented differently in the monolayer state. Moreover, compression-expansion cycling reveals that the poly(L-



lactide) and D/L blend monolayers differ in their kinetics, suggestive of differences in packing state. PM-IRRAS measurements establish that there is a difference between the conformation of the helical chains of the poly(L-lactide) and the D/L blend at the air–water-interface. The spectra reveal that with increased surface density, formation of poly(L-lactide) helices is occurring at the air–water interface.

**Acknowledgment.** This research was supported by Research Grants from NSERC (Canada) to G.R.B., R.B.L., and M.P. J.M.K. thanks Sigma Xi, the Scientific Research Society, for a Grant-in-Aid of Research. R.B.L. acknowledges Merck Frosst Canada for support of aspects of this research.

LA020606W